

NO-A191 588

III-V TRANSISTORS FOR MM-WAVE APPLICATIONS(U) NAVNL
OCEAN SYSTEMS CENTER SAN DIEGO CA J R ZEIDLER ET AL
DEC 87

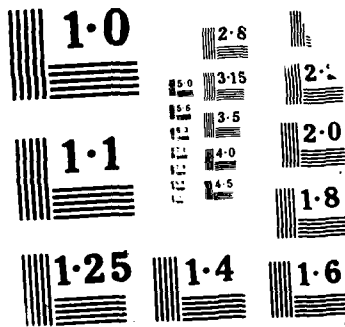
1/1

UNCLASSIFIED

F/G 9/1

NL







REPORT DOCUMENTATION PAGE

AD-A191 580

2b. DECLASSIFICATION/DOWNGRADING SCHEDULE		1b. RESTRICTIVE MARKINGS	
4. PERFORMING ORGANIZATION REPORT NUMBER(S)		3. DISTRIBUTION/AVAILABILITY OF REPORT Approved for public release; distribution is unlimited.	
6a. NAME OF PERFORMING ORGANIZATION Naval Ocean Systems Center	6b. OFFICE SYMBOL (if applicable) NOSC	7a. NAME OF MONITORING ORGANIZATION Naval Ocean Systems Center	
6c. ADDRESS (City, State and ZIP Code) San Diego, California 92152-5000		7b. ADDRESS (City, State and ZIP Code) San Diego, California 92152-5000	
8a. NAME OF FUNDING/SPONSORING ORGANIZATION Defense Advance Research Project Agency	8b. OFFICE SYMBOL (if applicable) DARPA	9. PROCUREMENT INSTRUMENT IDENTIFICATION NUMBER	
8c. ADDRESS (City, State and ZIP Code) Defense Sciences Office 1400 Wilson Blvd. Arlington, VA 22209		10. SOURCE OF FUNDING NUMBERS	
		PROGRAM ELEMENT NO. 61101E	TASK NO. EE66
			AGENCY ACCESSION NO. ICEE6 6B0
11. TITLE (include Security Classification) III-V Transistors for MM-Wave Applications			
12. PERSONAL AUTHOR(S) J. R. Zeidler			
13a. TYPE OF REPORT Professional paper/speech	13b. TIME COVERED FROM Oct 1987 TO Oct 1987	14. DATE OF REPORT (Year, Month, Day) December 1987	15. PAGE COUNT
16. SUPPLEMENTARY NOTATION			
17. COSATI CODES		18. SUBJECT TERMS (Continue on reverse if necessary and identify by block number)	
FIELD	GROUP	SUB-GROUP	
		satellite-to-satellite communications	
		GaAs	
		MESFET	
19. ABSTRACT (Continue on reverse if necessary and identify by block number)			
<p>The ability to operate at frequencies at and above 60 GHz is desirable in many applications to increase bandwidth, achieve more favorable tradeoffs between antenna beamwidth and size, and to exploit frequency dependent transmission properties of the atmosphere. Corresponding device and circuit requirements are delineated. One especially demanding requirement is to develop phased arrays at 60 and 94 GHz. At 94 GHz this requires an array of transmit/receive (T/R) modules with center to center spacings of 1.5 mm between modules. Generating the required output power without exceeding thermal dissipation limits places stringent requirements on the solid state components of the T/R module.</p> <p>The first 60 GHz transistor amplifier was developed in 1983 using GaAs MESFETs. The DARPA Strategic Technology Office quickly initiated a program to extend these capabilities to develop a 60 GHz T/R module for satellite-to-satellite communications applications. Concurrently, in expectation that MESFET performance might prove inadequate for some EHF applications, the DARPA Defense Sciences Office initiated a program to develop alternative EHF transistor technologies. Various planar and vertical device structures have been fabricated and devices with measured gain at 94 GHz and projected values of the maximum frequency of oscillation, f_{max} up to 220 GHz have been developed under this program and others</p> <p>Presented at 1987 IEEE GaAs IC Symposium.</p>			
20. DISTRIBUTION/AVAILABILITY OF ABSTRACT <input type="checkbox"/> UNCLASSIFIED/UNLIMITED <input checked="" type="checkbox"/> SAME AS RPT <input type="checkbox"/> DTIC USERS		21. ABSTRACT SECURITY CLASSIFICATION UNCLASSIFIED	
22a. NAME OF RESPONSIBLE INDIVIDUAL J. R. Zeidler	22b. TELEPHONE (include Area Code) 619-553-1581	22c. OFFICE SYMBOL Code 7602	

DTIC ELECTE
MAR 23 1988
S E



Accession For

NTIS GRA&I
DTIC TAB
Unannounced
Justification

III-V TRANSISTORS FOR MM-WAVE APPLICATIONS

J. D. Murphy⁺ and J. R. Zeidler^{*}

⁺ DARPA Defense Sciences Office, Arlington, VA 22209

^{*} Naval Ocean Systems Center, Code 7601, San Diego, CA 92152-5000

By _____
Distribution/
Availability Codes

Dist	Avail and/or Special
A-1	

Introduction

The ability to operate at frequencies at and above 60 GHz is desirable in many applications to increase bandwidth, achieve more favorable tradeoffs between antenna beamwidth and size, and to exploit frequency dependent transmission properties of the atmosphere. Table 1 provides a listing of important requirements for EHF radar, communications and electronic warfare systems. Corresponding device and circuit requirements are delineated. One especially demanding requirement is to develop phased arrays at 60 and 94 GHz. At 94 GHz this requires an array of transmit/receive (T/R) modules with center to center spacings of 1.5 mm between modules. Generating the required output power without exceeding thermal dissipation limits places stringent requirements on the solid state components of the T/R module.

The first 60 GHz transistor amplifier was developed in 1983 using GaAs MESFETs (1). The DARPA Strategic Technology Office quickly initiated a program to extend these capabilities to develop a 60 GHz T/R module for satellite-to-satellite communications applications. Concurrently, in expectation that MESFET performance might prove inadequate for some EHF applications, the DARPA Defense Sciences Office initiated a program to develop alternative EHF transistor technologies. Various planar and vertical device structures have been fabricated and devices with measured gain at 94 GHz and projected values of the maximum frequency of oscillation, f_{max} , up to 220 GHz have been developed under this program and others.

PRESENT CAPABILITIES OF MM-WAVE POWER TRANSISTORS

The frequency where the short circuit current gain of a FET equals unity, f_T is given by

$$f_T = \frac{g_m}{2\pi C_{sg}} = \frac{v_s}{2\pi L_g}$$

where g_m is the transconductance, C_{sg} is the source to gate capacitance, v_s is the saturated electron velocity, and L_g is the gate length. The frequency at which the maximum available power gain of the device equals unity is equal to f_{max} and is related to f_T by an expression which contains the parasitic resistances and reactances of the device.

A common method of increasing f_T and f_{max} is to scale the device size downward by reducing L_g .

Recent developments in electron beam lithography allow the fabrication of planar devices with L_g as small as 0.1 (Ref. 2). As discussed in Reference 3 however the thickness, a , of the conduction channel of the device must be reduced as L_g is decreased in the ratio $L_g/a > 3$ to ensure that current pinch-off can be maintained. As reported in Reference 2, the output conductance of MESFETs is observed to increase as L_g is decreased from 1μ to 0.1μ due to current leakage through the semi-insulating substrate and difficulty in achieving optimal scaling of the channel thickness to maintain pinch-off conditions. As the channel thickness is decreased, the doping density in the channel must be correspondingly increased to maintain channel current and output power. As the concentration of dopants increases beyond the mid 10^{17} ions/cm³ range, two factors combine to degrade performance. First, impurity scattering from ionized donors reduces the saturated electron velocity. Second, the breakdown voltage of the device is decreased due to the high electric fields at the Schottky metal-semiconductor interface. In spite of these difficulties, MESFETs with 6.5 db gain at 60 GHz (Ref. 4) and oscillation frequencies of 115 GHz (Ref. 5) have been reported. As shown in Reference 6 however, the power density and efficiency of GaAs MESFETs degrade rapidly at frequencies greater than 44 GHz.

A vertical FET (VFET) structure which eliminates current leakage through the substrate was developed at Westinghouse R&D center under DARPA funding (7). Westinghouse demonstrated the complex technologies required to etch vertical channels, place gates on the vertical sidewalls and interconnect the gate metals. A gain of 11.3 db at 18 GHz and an extrapolated f_{max} of 67 GHz was achieved. The device also demonstrated lower output conductance and lower feedback capacitance than a comparable MESFET. In addition the device is 20 times smaller than an equivalent FET which could, in principle, provide more efficient power combining techniques.

To increase the breakdown voltage of GaAs FETs, an undoped layer of AlGaAs has been placed under the gate metal to provide a MISFET-like device (8,9). This device generated 320 milliwatts of output power with a power density of 1 watt/mm and an efficiency of 33% at 18.5 GHz (8). MISFET devices with quantum wells are now under development for 60 and 94 GHz under DARPA sponsorship. The development of high electron mobility transistors (HEMT) (also called MODFETs, et al) has

Table 1. Representative device and circuit requirements for millimeter wave applications.

System Requirement	Device Requirements		Circuit Requirements
	Operating Conditions	Critical Parameters	
1. EHF Receiver	<ul style="list-style-type: none"> Low noise figure gain ≥ 3 dB 	<ul style="list-style-type: none"> High f_t, f_{max} Large g_m's Small device dimensions Small parasitics Small contact resistances 	<ul style="list-style-type: none"> Small dimensions Minimize transmission losses Noise matched input stage Monolithic technology desirable
2. EHF High Power Transmitter	<ul style="list-style-type: none"> High operating voltage, current, gain, and efficiency 	<ul style="list-style-type: none"> All parameters above plus maximum power gain High breakdown voltage Low output conductance, capacitance Low common lead inductance Low thermal resistance Low substrate leakage 	<ul style="list-style-type: none"> Optimum load match Low loss cell, device power combiners Low thermal resistance Monolithic technology High yield required due to increased size
3. High Power High Bandwidth Transmitter eg. BW $\approx 10\%$ for comm. 10-20% for radar, multioctave for EW	<ul style="list-style-type: none"> High gain, bandwidth product (f_{max}) 	<ul style="list-style-type: none"> Same as 1 and 2 	<ul style="list-style-type: none"> Broadband power combiner Distributed amplifier Monolithic technology High yield
4. High Reliability	<ul style="list-style-type: none"> Stable Ohmic and Schottky Contacts High breakdown voltage Radiation hardness Electrostatic discharge resistance Minimum diffusion rate between layers Low junction temperature Thermal shock cycling 		<ul style="list-style-type: none"> Integrity of interconnects Mechanical strength Low thermal resistance Monolithic integration

provided a significant breakthrough in EHF devices. HEMTs place the donor atoms in a wider bandgap layer such as a GaAlAs layer which is separated from an undoped GaAs layer by a thin buffer layer which shields the undoped GaAs conduction channel from the electrostatic potential in the donor layer with minimal reduction in the electron transfer efficiency between the doped and undoped layers. The development of improved epitaxial growth capabilities using molecular beam epitaxy has allowed the development of single and multiple heterojunction devices with uniform doping concentrations, uniform thickness, and sharp transitions between layers. The conduction band discontinuity between the doped AlGaAs and undoped GaAs layers localizes the carriers to a thin ($<100\text{\AA}$) layer in the undoped GaAs near the heterojunction interface. The low impurity scattering in this channel provides much higher transconductance than MESFETs of comparable dimensions. HEMT devices have also demonstrated increased output conduction due to the improved carrier confinement (6). Further improvements have been obtained using a heterojunction of doped AlGaAs and undoped InGaAs grown on an undoped GaAs buffer on a semi-insulating GaAs substrate (10). This InGaAs/AlGaAs pseudomorphic HEMT was shown to provide improved carrier confinement, higher transconductance, higher current levels, higher breakdown voltage, and reduced source resistance over conventional HEMTs due to the more favorable transport properties and the larger conduction band discontinuity. At 60 GHz a conventional HEMT has demonstrated a power density of 0.41 watts/mm with 14% power added efficiency. Pseudomorphic HEMTs of comparable dimensions have provided 0.43 watts/mm with 28% power-added efficiency at 60 GHz and 0.17 watts/mm with 10% efficiency at 93 GHz. The highest reported output power for any EHF device is 50 mwatts at 60 GHz and 9 mwatts at 94 GHz for single heter-

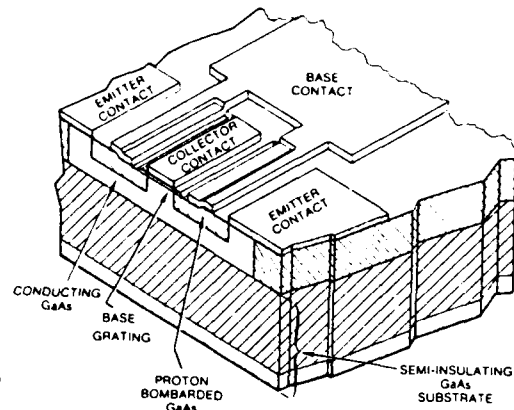


Figure 1. PBT on semi-insulating substrate.

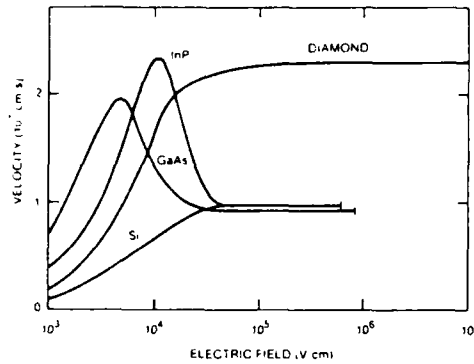


Figure 2. Steady-state velocity-field characteristics for various materials.

ojunction pseudomorphic and conventional HEMTs. The fact that the measured output power of HEMT devices has exceeded that of comparable FETs at 60 GHz was an unexpected result due to the relatively low sheet carrier density and the low breakdown voltages of early HEMT devices. Work is currently underway to achieve higher output power from HEMTs using various alloy combinations, multiple heterojunctions and increased gate widths. The MESFET and HEMT are horizontal devices where current flow is parallel to the surface and the critical control dimension is established by fine line lithography. By contrast, in vertical device structures the length of the control region in the direction of current flow which limits device speed is determined by layer thickness. Since with MBE or MOCVD, epitaxial layer thickness can be controlled to almost monatomic dimensions (several angstroms) the inherent speed potential of vertical devices is obvious. This class of devices comes with its own set of processing challenges. The development of materials and processing technology to realize vertical EHF three-terminal device concepts has been a major emphasis of the DARPA program since its inception. Currently the most mature vertical transistors, the permeable base transistor (PBT) and the heterojunction bipolar transistor (HBT), have already demonstrated extrapolated f_{max} in excess of 200 GHz and 100 GHz respectively. The GaAs PBT (11) is a majority carrier device in which holes do not participate in current flow.

It could be considered as a multichannel vertical FET. However it is usually described in bipolar terminology. The emitter and collector regions (Fig. 1) are separated by a tungsten grating embedded in single crystal GaAs. A high breakdown voltage of around 20 volts is realized. The physical "gatelength" corresponds to the thickness of the tungsten grating lines and is typically about 300 angstroms (0.3 microns), whereas for FET's and HEMT's, it is only recently that .1 micron L_g devices have been achieved. The emitter to collector spacing in the PBT can be made as short as .25 microns or less; comparable short source to drain spacings are difficult to achieve in FET's and HEMT's. Being a vertical device with many adjacent channels, the PBT does not suffer from the substrate leakage problems inherent to horizontal devices and consequently has high output impedance. Another potential advantage is its compactness. For example, an 80 x 40 micron PBT is equivalent to a 2 mm gatewidth FET. The more compact geometry of a PBT means that it can control large currents without the gate voltage distribution problems (phasing) at EHF frequencies of conventional devices. Unknown at present are thermal management problems that might accompany the compact geometry of the PBT.

The critical step in PBT fabrication, overgrowth of single crystal GaAs on a tungsten grating, is done by MOCVD. Devices with f_{max} in excess of 100 GHz can now be routinely processed. The grating can be defined by e-beam or x-ray lithography and there is no critical alignment with any other wafer feature required in the entire device process sequence; the most stringent alignment is aligning a 4 micron wide collector ohmic contact in the 8 micron gap between base contact pads. Recent PBT results (12, 13) indicate maximum stable power gain (MSG) values of 21.3 dB at 18 GHz and 15 dB at 40 GHz. These values are believed to be the highest values ever reported for any three-terminal device. Assuming a rolloff in power gain of 6dB/octave, an extrapolated f_{max} of around 220 GHz was obtained. A power-added efficiency of 41% was measured in class AB operation of a PBT at 20 GHz, a result thought to be a record (14). Additionally, an electro-optic measurement (15) of PBT turn-on risetime at room temperature yielded 5 psec -- the shortest risetime yet measured for any transistor. A minor design change is being incorporated to enable growth of PBT's on semi-insulating GaAs. To optimize device power output, modifications to the doping profile, collector contact geometry, and wafer thickness are in progress.

The idea of a widegap emitter bipolar transistor originated with W. Shockley (16). The GaAs/GaAlAs HBT has been grown by MOCVD as well as MBE and excellent results have been obtained on silicon substrates; this is potentially important for GaAs-based mmwave phased arrays because of the superior thermal conductivity (as well as large area and robustness) of silicon. As Kroemer (16) has pointed out, the HBT benefits from the "Central Design Principle" of heterostructure devices, i.e., the use of a combination of energy gaps and electric fields to independently control the forces on electrons and holes. Simplified theory predicts that the f_{max} of a bipolar transistor is given by

$$f_{max}^2 = Ft / 8\pi R_b C_{cb}$$

with R_b = base resistance, and C_{cb} = collector-base capacitance. Using a heavily doped base, a fully self-aligned process, and optical lithography, npn devices with emitter width of 1.2 micron have yielded an extrapolated f_{max} of 105 GHz (17). The HBT is unique among candidate mmwave devices in that it may be fabricated with conventional optical lithography. To increase f_{max} , base resistance must be lowered and collector capacitance decreased. An intriguing possibility that DARPA is evaluating for lowering R_b is to incorporate a metal grating in the base, a technology already developed for the PBT. In an inverted structure with a topside collector, C_{cb} can in principle be lowered. Major challenges to fabrication of such a structure include collector contacts capable of withstanding high temperature base annealing, and a well controlled dry etching technology. For a collector width of .5 micron, an inverted npn GaAs/GaAlAs HBT is projected to have an f_{max} of over 300 GHz. Power densities of HBT's at 10 GHz are two to four times those of FET's and packing densities are five to ten times better. As with PBT's, thermal and reliability issues concerning mmwave HBT's remain to be explored.

PROSPECTS FOR HIGH POWER EHF TRANSISTORS

The rapid improvement in planar EHF device performance has been due to the significant improvements in electron beam lithography, epitaxial growth, dry etching, rapid thermal annealing, and ohmic contact technologies. These technologies have enabled fabrication of multiple heterojunction devices with shorter gate lengths and dramatically improved transconductance, carrier velocities, and improved carrier confinement. Performance of vertical devices will continue to improve as advances in fabrication technology allow the inherent advantages of short conduction channels to be exploited. Such devices will be especially important in the realization of hot electron devices where carriers move through the device at ballistic speeds without scattering (18). Ballistic injection and drift transistors are currently being investigated under DARPA funding. Calculations have shown that hot electron effects must be included to explain the measured performance data of AlGaAs/GaAs HBTs (19). Continued improvements are expected as new materials and alloy combinations are utilized to optimize carrier concentrations and transport properties and to minimize parasitic losses and increase breakdown voltage (20).

The transconductance and f_T are strong functions of the electric field dependent velocity, $v(E)$, of the charge carriers. Comparative electron velocities as a function of electric field for Si, GaAs, InP and Diamond are shown in Figure 3 (21). InP offers high peak electron velocities and higher velocities at moderate fields due to the greater separation of the γ -L valleys in the conduction band and the higher threshold field for intervalley electron transfer (22). InP also provides improved thermal conductivity relative

to GaAs. At 9.7 GHz, an InP MISFET has recently demonstrated 4.5 watts output power with 4 dB gain at 46% power added efficiency and 4.5 watts/mm of gate width, over 3 times the highest power density reported for a GaAs FET (23). InP device technology would also allow integrated optoelectronics for long wavelength optical communications (24). Bipolar devices are also being grown on InP substrates to obtain increased current gain at low collector current levels (25, 26). This results from the lower surface recombination currents in InGaAs/InP devices relative to AlGaAs/GaAs. In addition the growth of InAlAs/InGaAs HEMTs on InP allows more desirable alloy compositions to be fabricated without the large strain which results when these materials are grown on GaAs (27). InP technology is immature compared to GaAs, however, and a significant investment is needed to enable widespread application of InP devices and integrated circuits.

As indicated in Figure 3, $v(E)$ behavior of semi-conducting diamond offers dramatically superior transport properties at high fields. Diamond also provides low thermal resistance, high radiation hardness, and high strength and corrosion resistance. Recent achievements in the growth of conducting diamond films (28) could lead to high performance EHF devices provided that the significant challenges of large area crystalline growth and controlled introduction and activation of dopants at desired operating temperatures can be accomplished.

REFERENCES

1. E. Watkins, et al, IEEE MTT-S Digest p. 145, 1983.
2. H. Jaekel, et al, IEEE Electron Device Letters, EDL-7, p. 522, 1986.
3. H. Daembkes, et al, IEEE Trans Electron Devices, ED-31, p. 1032, 1984.
4. B. Kim, et al, EDL-6, p. 1, 1985.
5. H. Q. Tserng and B. Kim, IEEE GaAs Symposium Digest, p. 11, 1985.
6. P. Smith, et al, IEEE MTT-S Digest, p. 749, 1987.
7. R. Clarke, et al, GOMAC Digest Papers, Vol XII, p. 75, 1986.
8. B. Kim, et al, IEEE Electron Device Letters, EDL-7, p. 638, 1986.
9. H. Hida, et al, EDL-7, p. 625, 1986.
10. T. Henderson, et al, EDL-7, p. 645, 1986.
11. C. Bozler and G. Alley, Proc IEEE, 70, p. 46, 1982.
12. R. Actis, et al, FDL-8, p. 86, 1987.
13. R. Murphy and J. Murphy, Microwave Journal p. 101, July 1987.
14. K. Nichols, et al, to be published.
15. D. Dykaar, et al, Proc Conf. Ultrafast Phenomena, p. 103, 1986.
16. H. Kroemer, Proc IEEE, 70, p. 13, 1982.
17. P. Asbeck, et al, to be published.
18. M. Heiblum and L. Eastman, Scientific American p. 102, Feb 1987.
19. Y. Yamauchi and T. Ishibashi, EDL-7, p. 655, 1986.
20. S. Krishnamurthy and A. Sher, J. Appl. Phys 61, p. 1475, 1987.
21. M. Geis, et al, EDL-8, p. 341, 1987.
22. C. Hansen, et al, EDL-8, p. 53, 1987.
23. L. Messick, et al, Proc. of the International Electron Devices Meeting, p. 767, 1986.
24. C. Cheng, et al, EDL-7, p. 549, 1986.
25. W. Lee & C. Fonstad, EDL-7, p. 549, 1986.
26. R. Nottenburg, et al, EDL-7, p. 643, 1986.
27. C. Peng, et al, EDL-8, p. 24, 1987.
28. N. Fujimori, et al, Vacuum, Vol 36, p. 99, 1986.

END

DATE

FILMED

DTIC

6-88